Spatial Self-Organization of Surface Structure during an Oscillating Catalytic Reaction

M. P. Cox, G. Ertl, and R. Imbihl
Institut für Physikalische Chemie, Universität München, 8 München 2, Federal Republic of Germany
(Received 3 July 1984)

Under appropriate conditions, the rate of catalytic CO oxidation on a Pt(100) surface exhibits sustained temporal oscillations which are associated with a periodic surface-structural transformation from the reconstructed (hex) to the nonreconstructed (1×1) phase and back again. By use of a newly developed scanning low-energy electron-diffraction technique it is demonstrated that spatial self-organization in the oscillations involves a wavelike propagation of alternating bands of the two surface-structural modifications across the entire scanned area. These features can be modeled by numerical solution of a set of coupled differential equations.

PACS numbers: 82.65.Jv, 68.45.Da, 82.20.Mj

The observation of temporal oscillations in the rate of catalytic CO oxidation, $CO+\frac{1}{2}O_2\rightarrow CO_2$ on Pt(100), under conditions (P_{CO},T) giving a critical CO coverage of $\frac{1}{2}$ monolayer (if this gas were present alone) led to the suggestion that this effect is associated with a periodic variation in the surface structure.[1] Attempts to detect this structural variation by Rutherford backscattering were unsuccessful,[2] probably because optimum conditions could not be established. However, the LEED pattern was indeed found to switch periodically between that of the reconstructed (hex) phase and that of the $c(2\times2)$ structure formed by half a monolayer of adsorbed CO on the nonreconstructed (1×1) Pt(100) surface.[3] Additionally the reaction rate had been found to be paralleled by changes of the work function $(\Delta\phi)$ averaged over the whole surface area (~ 20 mm^2) which suggests that also spatial self-organization of the structural transformation is associated with the kinetic oscillations. In this Letter it will be demonstrated how this latter effect could be experimentally verified, and in addition the features of a mathematical model for an appropriate description of the observed phenomena will be sketched.

In order to monitor any changes in the surface structure (as reflected by the LEED pattern) across the surface, a novel scanning technique was developed. The LEED primary electron beam (40 eV, 0.1 μA, 0.7 mm diameter) can be deflected across the crystal surface by means of two perpendicular pairs of Helmholtz coils, controlled by two coupled ramp generators. This setup allows a line scan of a few seconds duration across the crystal or alternatively a raster over an area approximately 7 mm$\times$4 mm with ten lines each of 1-sec duration. The complete LEED pattern is recorded continuously with a video camera during repeated scans of the electron beam. The intensities of up to four characteristic LEED spots may be measured and stored in an LSI11/23 computer every 0.1 sec,[4] thus giving 100 intensity points per raster frame. After corrections for variations in angle of incidence, beam current, and background effects (all arising from the changing magnetic field), the spot-intensity data can be plotted out as a function of time and of position on the surface.

Kinetic oscillations with large $\Delta\phi$ amplitudes (~ 300 meV) were established under continuous-flow conditions typically with $p_{CO}=5\times10^{-5}$ Torr, $p_{O_2}=5\times10^{-4}$ Torr at 480 K. Extreme care had to be taken with respect to gas purity and surface cleanliness, monitored by mass spectrometry and Auger-electron spectroscopy, respectively. Once the oscillations were established, they could be sustained for periods of up to several hours. Their wave form and periodicity, however, were sometimes markedly different from run to run for reasons which have not yet been clearly established. The period ranged from 30 to 100 sec for the conditions indicated above.

Figure 1 shows typical data from a LEED line-scan experiment, namely the intensity of the $(\frac{1}{2}\,\frac{1}{2})$ beam from the $c(2\times2)$-1×1 structure along a 6-mm line on the surface at various times. The variation of the intensity at a fixed point with time shows the typical oscillatory behavior as reported previously.[3] Comparison

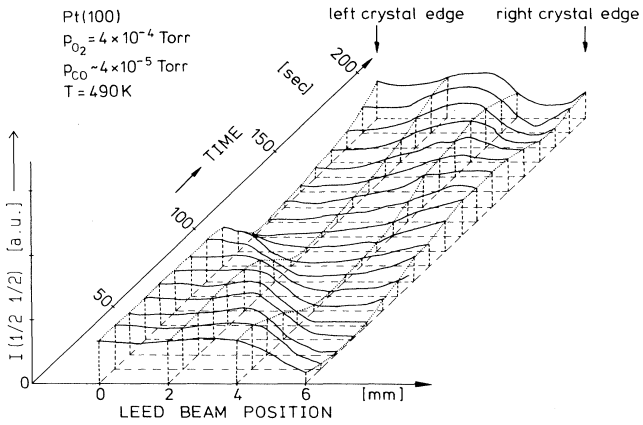

FIG. 1. LEED line-scan data taken during kinetic oscillations: intensity variation (arbitrary units) of the $c(2\times2)$ LEED pattern as a function of surface position and time. Time to scan one line = 4.7 sec.

of the data at different points on the surface demonstrates that the structural transformation does not occur everywhere in phase, but rather propagates as a wave from right to left.

This effect is even more striking in Fig. 2 which shows a series of two-dimensional intensity distributions taken at intervals of 10 sec for the $c(2\times2)$-1×1 and the hex structures simultaneously. These patterns complement each other, i.e., regions with high $c(2\times2)$-1×1 intensity are associated with low hex intensities and vice versa, as could also be seen by visual inspection of the LEED screen. The wave front of the structural transformation propagates (in this case) with a rate of about 0.2 mm/sec across the whole surface area of the sample. It appears as if these waves originate at the edges of the crystal, which exhibit a high degree of structural imperfection.

Similar scanning-LEED experiments have shown under all conditions investigated so far that kinetic oscillations on Pt(100) are associated with the appearance of spatial structures. Additionally, the *I-V* curves of the integral order beams, which can be used as a fingerprint for identification of different surface structures, showed no new features that could be attributed to intimately coadsorbed CO and O. It can be concluded that the two reactant species are located in different domains of macroscopic size on the surface. That part of the surface displaying only $c(2\times2)$-1×1 spots is simply a CO-covered 1×1 surface, whereas O is adsorbed on 1×1 patches which are dispersed between (essentially adsorbate-free) hex islands on a scale which is resolved by the LEED beam. Thus, under oscillatory conditions, a phase separation of the adsorbed CO and O takes place, detectable as a spatial structure in our scanning-LEED experiments.

From previous experimental and theoretical work on the catalytic CO oxidation[5] it is well known that for given p_{O_2}/p_{CO} and T, a multiplicity of the CO_2 production rate r can exist in which the state with lower r is connected with a high CO coverage of the surface and the state with higher r is connected with a low CO coverage. The LEED experiments described here have shown that at the minimum of $\Delta\phi$ in the oscillations most of the surface is covered by CO whereas at the maximum in $\Delta\phi$ the CO coverage is low. Thus the surface changes its catalytic activity during one cycle, this explaining the previous observation that CO_2 production rate and work function vary in parallel.[1]

The evolution of spatial patterns in chemically interacting systems has already been extensively studied with homogeneous reactions in solution, in particular with the famous Belousov-Zhabotinsky reaction.[6] The oscillatory kinetics of this complicated reaction sequence can be successfully modeled by a system of nonlinear, coupled differential equations including an autocatalytic step.[7] Spatial pattern formation (in the

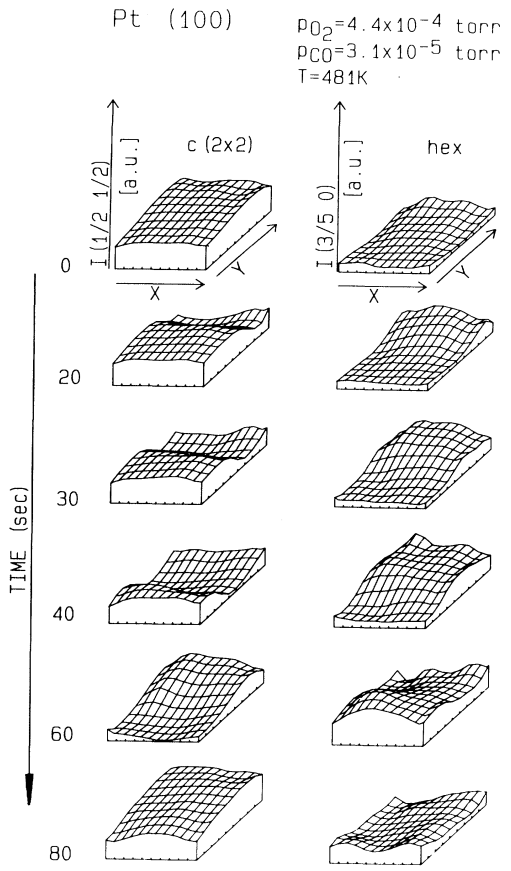

FIG. 2. LEED raster-scan data taken during kinetic oscillations: intensity variation of the $c(2\times2)$ and hex LEED patterns as a function of surface position and time. Time to scan one frame (of ten lines) = 10.0 sec. Size of scanned area = 4 mm in X and 7 mm in Y direction. Crystal surface: elliptical, minor axis 6.5 mm, major axis 9 mm, major axis parallel to Y.

form of concentric rings or spirals) may take place through propagation of "trigger waves" created at small regions of disturbance.[8] More generally these phenomena can be described[9] by a set of coupled reaction/diffusion equations of the form $\mathbf{q}(\mathbf{x},t) = R(\mathbf{q}(\mathbf{x},t),\mathbf{x},t) + D\Delta\mathbf{q}(\mathbf{x},t)$, where $\mathbf{q}$ denotes the concentration variables. The function R describes the dependence of the reaction rate on $\mathbf{q}$, position $\mathbf{x}$, and time t, while the last term represents diffusion.

The mechanism of catalytic CO oxidation on platinum is well established and proceeds through the following steps[10]:

$$CO + * \rightleftarrows CO_{ad},\quad O_2 + * \rightarrow 2O_{ad},\quad CO_{ad} + O_{ad} \rightarrow CO_2.$$

The properties of the hex and 1×1 phases of the Pt(100) surface differ considerably from each other. The heats of CO and O_2 adsorption are higher on the 1×1 phase (which is the driving force for the

adsorbate-induced hex → 1×1 transformation), while on the other hand the clean hex surface is energetically more stable than the clean 1×1 surface.[11] The oxygen sticking coefficient on the hex surface is by at least 2 orders of magnitude smaller than on the 1×1 phase.[12] On the basis of this independently obtained information the present system could be successfully modeled by a system of equations describing the variations of coverages and the structural changes of the surface as function of time t and of space x. In this one-dimensional model the surface was divided into forty compartments each of length 0.01 cm giving a total length of 0.4 cm. The fractions of the surface area present in the 1×1 and hex structures were denoted by a and b, respectively. The local coverages of CO on 1×1 and hex patches are denoted by U_a and U_b, respectively, and the respective O coverages by V_a and V_b. The coverages averaged over each of the individual compartments are denoted by $u_a = aU_a$, $u_b = bU_b$, etc., and we then arrive at the following set of coupled differential equations:

$$\partial u_a/\partial t = k_1 a p_{CO} - k_2 u_a + k_3 a u_b - k_4 u_a v_a/a + k_5 \partial^2(u_a/a)/\partial x^2, \tag{1}$$

$$\partial u_b/\partial t = k_1 b p_{CO} - k_6 u_b - k_3 a u_b, \tag{2}$$

$$\partial v_a/\partial t = k_7 a p_{O_2}([1 - 2u_a/a - 5v_a/3a]^2 + \alpha[1 - 5v_a/3a]^2) - k_4 u_a v_a/a, \tag{3}$$

$$\partial a/\partial t = \begin{cases} (1/U_{a,\mathrm{grow}})\partial u_a/\partial t, & \text{if } U_a = u_a/a > U_{a,\mathrm{grow}} \approx 0.4\text{–}0.5, \quad (4a) \\ -k_8 ac, & \text{if } c = U_a/U_{a,\mathrm{crit}} + V_a/V_{a,\mathrm{crit}} < 1, \quad (4b) \\ 0, & \text{otherwise.} \quad (4c) \end{cases}$$

Equations (1) and (2) describe the variation of the amounts of CO adsorbed on the 1×1 and hex phase by adsorption, desorption, surface reaction, and diffusion, respectively. Equation (3) is the analogous expression for O on the 1×1 surface. The terms in square brackets allow for the inhibition of oxygen adsorption by the presence of adsorbed particles. The term with k_5 accounts for the enhanced adsorption rate at defects, which are present, e.g., at the edges of the crystal. The coefficients (2 and $\frac{5}{3}$) in this equation arise from the experimental CO and O coverages at which further oxygen adsorption on Pt(100) is inhibited: $U_a = \frac{1}{2}$, $V_a = \frac{3}{5}$. It is assumed that the defect sites are only blocked by O. Since the oxygen sticking coefficient on the hex phase is very small ($\sim 10^{-4}$) the corresponding equation for v_b can be neglected. Coupling between different regions on the surface is achieved by CO diffusion between the 1×1 areas via k_5. The term with k_3 describes trapping of CO at the 1×1 patches by migration from the hex phase due to the enhanced heat of adsorption. Equation (4a) describes the nonactivated hex → 1×1 transformation if the local CO coverage exceeds $U_{a,\mathrm{grow}}$. Equation (4b) holds for the situation where the combined CO and O coverages fall below the critical values ($U_{a,\mathrm{crit}} \approx 0.3$; $V_{a,\mathrm{crit}} \approx 0.4$) for the onset of the activated 1×1 → hex transition.

For numerical integration of these equations almost all parameters were known from independent experiments and a full account will be given elsewhere.[13] Figure 3 shows a sequence of resulting spatial patterns at various times which demonstrate the evolution of self-organizatoin during one oscillation cycle. In these calculations a higher α (reflecting a higher defect density) was associated with the three left-hand edge compartments which then act as triggers for the propagat-

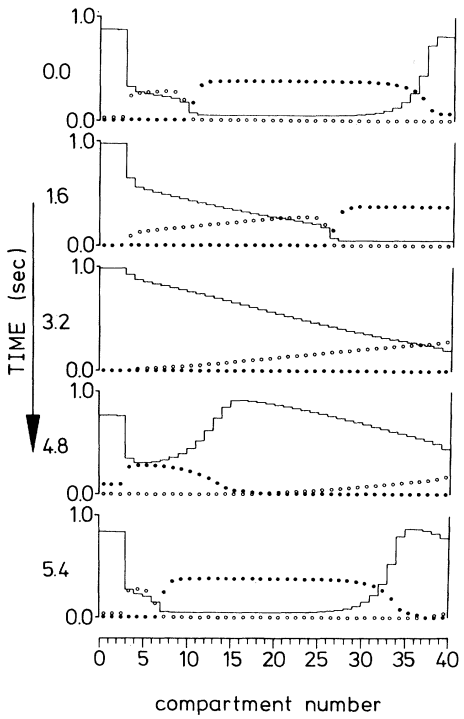

FIG. 3. Numerical integration of Eqs. (1)–(4) with parameters appropriate to $T = 480$ K, $p_{CO} = 9.0 \times 10^{-6}$ Torr, $p_{O_2} = 2.0 \times 10^{-4}$ Torr. Forty compartments each of width 10^{-2} cm. $k_1 p_{CO} = 2.1$ ML s^{-1}; $k_2 = 1.5$ s^{-1}; $k_3 = 50$ s^{-1}; $k_4 = 10^4$ ML^{-1} s^{-1}; $k_5 = 4.0 \times 10^{-4}$ cm^2 s^{-1}; $k_6 = 11$ s^{-1}; $k_7 p_{CO} = 11$ ML s^{-1}; $k_8 = 1.9$ s^{-1}; $U_{a,\mathrm{grow}} = 0.4$ ML; $U_{a,\mathrm{crit}} = 0.32$ ML; $V_{a,\mathrm{crit}} = 0.4$ ML (ML = monolayer); $\alpha = 0.4$ for the three left-hand compartments; $\alpha = 0.1$ for the remaining compartments. Full line, b (hex structure); full circles, U_a (CO coverage on 1×1); open circles, V_a (O coverage on 1×1).

ing waves. Figure 3 obviously reflects all the qualitative features of the experimental data. The resulting period is, however, still shorter than the experimental one which is mainly caused by the fact that for computational reasons unrealistic high values for k_5 and k_8 were used for the calculations.

In conclusion, the system presented here represents the first example of a heterogenously catalyzed reaction for which temporal and spatial self-organization could be observed and could be traced back to transformations of the surface structure.

Financial support of this work by the Deutsche Forschungsgemeinschaft (Sonderforschungsbereich 128) and by the Royal Society is gratefully acknowledged.

[1]G. Ertl, P. R. Norton, and J. Rüstig, Phys. Rev. Lett. **49**, 177 (1982).

[2]P. R. Norton, P. E. Bindner, K. Griffiths, T. E. Jackman, J. A. Davies, and J. Rüstig, J. Chem. Phys. **80**, 3859 (1984).

[3]M. P. Cox, G. Ertl, R. Imbihl, and J. Rüstig, Surf. Sci. **134**, L517 (1983).

[4]E. Lang, P. Heilmann, G. Hanke, K. Heinz, and K. Müller, Appl. Phys. **19**, 287 (1979).

[5]J. M. White and A. Golchet, J. Catal. **53**, 266 (1978).

[6]See, e.g., R. M. Noyes and R. J. Field, Annu. Rev. Phys. Chem. **25**, 95 (1974).

[7]K. Showalter, R. M. Noyes, and K. Bar-Eli, J. Chem. Phys. **69**, 2514 (1978).

[8]A. T. Winfree, Faraday Symp. **9**, 38 (1974); R. J. Field and R. M. Noyes, Faraday Symp. **9**, 21 (1974).

[9]A. Haken, *Synergetics* (Springer-Verlag, Berlin, 1977), and *Advanced Synergetics* (Springer-Verlag, Berlin, 1983); P. H. Richter, I. Procaccia, and J. Ross, Adv. Chem. Phys. **43**, 217 (1980).

[10]G. Ertl, in *Catalysis, Science and Technology,* edited by J. R. Anderson and M. Boudart (Springer-Verlag, Berlin, 1983), p. 209.

[11]R. J. Behm, P. A. Thiel, P. R. Norton, and G. Ertl, J. Chem. Phys. **78**, 7437, 7448 (1983); T. E. Jackman, K. Griffiths, J. A. Davies, and P. R. Norton, J. Chem. Phys. **79**, 3529 (1983).

[12]M. A. Barteau, E. I. Ko, and R. J. Madix, Surf. Sci. **102**, 99 (1981), and **104**, 161 (1981); P. R. Norton, K. Griffiths, and P. E. Bindner, Surf. Sci. **138**, 125 (1984).

[13]R. Imbihl, M. P. Cox, G. Ertl, H. Müller, and W. Brenig, J. Chem. Phys. (to be published).